Journals of Gerontology: BIOLOGICAL SCIENCES
Cite journal as: J Gerontol A Biol Sci Med Sci 2014 July;69(7):810–820
doi:10.1093/gerona/glt210

Advance Access publication January 7, 2014

Effects of Lithium on Age-related Decline in Mitochondrial Turnover and Function in *Caenorhabditis elegans*

Zhi Yang Tam,[1] Jan Gruber,[2,3] Li Fang Ng,[2] Barry Halliwell,[2] and Rudiyanto Gunawan[1]

[1]Institute for Chemical and Bioengineering, ETH Zurich, Switzerland.
[2]Department of Biochemistry, Centre for Life Sciences and
[3]Yale-NUS College, Science Division, National University of Singapore, Singapore.

Address correspondence to Rudiyanto Gunawan, PhD, Institute for Chemical and Bioengineering, ETH Zurich, Wolfgang-Pauli-Strasse 10, 8093 Zurich, Switzerland. Email: rudi.gunawan@chem.ethz.ch

Aging has been associated with the accumulation of damages in molecules and organelles in cells, particularly mitochondria. The rate of damage accumulation is closely tied to the turnover of the affected cellular components. Perturbing mitochondrial turnover has been shown to significantly affect the rate of deterioration of mitochondrial function with age and to alter lifespan of model organisms. In this study, we investigated the effects of upregulating autophagy using lithium in *Caenorhabditis elegans*. We found that lithium treatment increased both the lifespan and healthspan of *C. elegans* without any significant change in the mortality rate and oxidative damages to proteins. The increase in healthspan was accompanied by improved mitochondrial energetic function. In contrast, mitochondrial DNA copy number decreased faster with age under lithium. To better understand the interactions among mitochondrial turnover, damage, and function, we created a mathematical model that described the dynamics of functional and dysfunctional mitochondria population. The combined analysis of model and experimental observations showed how preferential (selective) autophagy of dysfunctional mitochondria could lead to better mitochondrial functionality with age, despite a lower population size. However, the results of model analysis suggest that the benefit of increasing autophagy for mitochondrial function is expected to diminish at higher levels of upregulation due to a shrinking mitochondrial population.

Key Words: *Caenorhabditis elegans*—Lithium—Mitochondria—Mathematical model—Aging.

Received June 17, 2013; Accepted November 28, 2013

Decision Editor: Rafael de Cabo, PhD

AGING is characterized by progressive deterioration of an organism at all levels (genetic, molecular, cellular, and organismal), weakening its ability to maintain homeostasis (1). Aged cells accumulate damaged macromolecules (eg, lipofuscin, aberrant proteins, and protein aggregates) and have reduced energetics due to dysfunctional mitochondria (2). The build-up of damaged molecules and organelles coincides with a reduction in protein and mitochondrial turnover processes (2) and is thought to play a role in the pathogenesis of age-related diseases. The relationship between damage accumulation and aging and age-related diseases is the basis for damage-based theories of aging (3).

The key target organelles of damage accumulation in this context are mitochondria. Although the main role of mitochondria is to carry out cellular respiration through oxidative phosphorylation, these organelles are also involved in a wide range of regulatory processes that are vital to cellular homeostasis, such as iron metabolism, fatty acid oxidation, apoptosis, cell cycle, and cell signaling (4). Mitochondrial function declines with age (5), alongside with a decrease in mitochondrial DNA (mtDNA) and mitochondria-related mRNA abundance, and an increase in reactive oxygen species generation (6,7). This decline is also accompanied by a reduction in mitochondrial autophagy (mitophagy) (8) and mitochondrial biogenesis (mitogenesis) (9–11). Mitophagy in this study refers to both selective and nonselective degradation of mitochondria by the cellular autophagy system. The slowdown of mitochondrial turnover has been proposed to contribute to the deterioration of mitochondrial quality control and function, and consequently to contribute to the pathogenesis of age-related diseases and aging itself (2,12). Modulation of key parameters controlling mitochondrial turnover, function, and repair is therefore a promising target for interventions to the aging process (13–15).

In support of this approach, there is evidence in mice that perturbation of mitochondrial turnover can significantly affect mitochondrial function. For example, in a mouse model of mitochondrial myopathy, overexpression of peroxisome proliferator-activated receptor gamma coactivator 1-alpha (PGC-1α), a transcription co-activator involved in mitochondrial biogenesis (16), led to improved mitochondrial function (adenosine triphosphate [ATP] levels), delayed onset of myopathy, and prolonged lifespan (17). On the other hand, inhibiting autophagy has been shown to result in aging-like phenotypes, such as accumulation of lipofuscin-like material and dysfunctional mitochondria (18), increased

generation of reactive oxygen species (19), and symptoms of neurodegeneration in mice (20). In contrast, pharmacological intervention using rapamycin has been shown to upregulate autophagy (21) and extend the lifespan of mouse, worm, and fruit fly (22,23). Treatment with rapamycin has also been shown to permit a faster clearance of aberrant proteins, such as mutant huntingtin and α-synucleins (24,25).

Searching the literature for additional pharmacological modulators of mitophagy, we found *in vitro* evidence that lithium treatment upregulates autophagy (24). Lithium has been used for the treatment of bipolar disorder for over 100 years (26). The efficacy of lithium in treating bipolar disorder has been proposed to arise from its upregulation of neurotrophins such as brain-derived growth factor and nerve growth factor (27). Lithium is also a neuroprotective agent that prevents neuron apoptosis (28). In addition, lithium has also been shown to enhance the generation of pluripotent stem cells (29) and is capable of stimulating neurogenesis (30). These effects, along with the upregulation of autophagy by lithium (24), have motivated the use of lithium in the treatment of neurodegenerative diseases (31,32).

Lithium has previously been shown to increase ATP production in primary bovine aortic endothelial cells, in which such an increase was attributed to higher mitochondrial mass (33). Interestingly, lithium treatment has been reported to extend lifespan in *Caenorhabditis elegans* previously (22,34). Furthermore, the concentration of lithium in tap water was found to be inversely correlated with all-cause mortality in 18 different Japanese municipalities (34). However, in the study by McColl and colleagues (22), an altered expression of genes encoding nucleosome-associated functions was proposed to be responsible for the lifespan extension. Here, we explore if lithium treatment in *C. elegans* leads to increased autophagy and if this increase is associated with reduced damage accumulation with age and improved mitochondrial function. To this end, we examined the effects of lithium on *C. elegans* lifespan and healthspan, ATP production, mtDNA copy number, and oxidative damage. Given the complex and dynamic interplay between lithium-induced and age-related changes in cellular processes, we formulated a model of mitochondrial damage accumulation, describing the population balance of functional and dysfunctional mitochondria. We combined experiment and model-based analysis to gain a better understanding of nonintuitive trends in the experimental data and to lay any mechanistic explanation of lithium effects on a more quantitative ground.

Methods

Nematode Strains and Maintenance

The JK1107 (*glp-1*) and DA2123 (adIs2122[*lgg-1*:GFP rol-6(df)]) *C. elegans* strains were used in the lifespan study and the assessment of autophagy, respectively. The DA2123 strain was obtained from the *Caenorhabditis* Genetic Center (Minneapolis, MN). DA2123 worms were maintained at 20°C on nematode growth medium (NGM) agar plates, while JK1107 worms were cultivated at 25.5°C to prevent progeny. NGM was prepared as previously described (35) with an addition of streptomycin to a final concentration of 200 μg/mL. Streptomycin at this concentration exhibited no effect on the mitochondrial oxygen consumption of wild-type N2 worms (see Supplementary Figure S1). A discussion on the use of streptomycin in *C. elegans* lifespan studies is also included in the supplementary information. Streptomycin-resistant *Escherichia coli* strain OP50-1 was added to each plate (50 μL of 10^{10} cells/mL of *E coli* stock per plate).

Lithium Administration

Lithium chloride (LiCl) was dissolved in highly purified water to a final concentration of 10 mM and added to freshly autoclaved NGM just before solidification (55–60°C). In all experiments, synchronous cultures of worms were obtained from hypochlorite treatment (35). The worm eggs were allowed to hatch on control NGM plates that did not contain LiCl. Subsequently, worms in the lithium-treated group were transferred as young adult (Day 3 posthatching) to NGM plates in the presence of LiCl.

Lifespan and Motility Studies

JK1107 worms were cultivated at a permissive temperature of 16°C and moved to 25.5°C as eggs for the lifespan study. Populations of young adult worms (Day 3 posthatching) were transferred to plates with and without LiCl and counted every 1–3 days depending on the prevalent mortality. Worms that failed to respond to mechanical stimuli were scored as dead and removed from the plate. Worms that had crawled off onto the sides of the plate and died away from the agar were excluded from the analysis. The study was performed under blinded condition as described in the study by Schaffer and colleagues (13), where the control and treatment plates were randomly assigned a plate number by an operator unrelated to the lifespan experiment. Age-synchronized JK1107 worms were assessed both for spontaneous locomotion and response to prodding with a platinum wormpick, and their activity was scored as previously described (36).

Motility and Mortality Analysis

Using the survival curves of control and LiCl-treated worms obtained from blinded experiments, the linear region of the log mortality ($m(t)$) was used in the calculation of mortality with a discrete time interval of 2 days. The Gompertz function ($m(t) = Ae^{Gt}$), which describes the age-related exponential increase in mortality, was fitted

to these data to generate the estimates of the parameter *A*, which describes the age independent factor in mortality, and the parameter *G,* which describes the age-dependent, exponential increase in mortality. The mortality rate doubling time was subsequently calculated from *G*, according to $MRDT = \ln\left(\frac{2}{G}\right)$ (37).

Assessment of Autophagy

L4 DA2123 worms (Day 2 posthatching) were transferred to control and LiCl NGM plates. The plates were incubated at 20°C overnight. The worms were mounted onto a 5% agar pad with 1–2 μL of sodium azide as described in the study by Shaham (38) and imaged. Two sets of 35 images were acquired for control and lithium-treated worms, and the images (70 in total) were randomly labeled and scored by three operators unrelated to this study. The statistical significance was determined using a binomial test and only the highest *p*-value was reported.

ATP Assay

The ATP assay was performed as described in the study by Schaffer and colleagues (13). A population of 100 worms was collected in M9 buffer and washed three times to remove residual bacteria. After washing, the worms were flash frozen using liquid nitrogen and stored in −80°C. For the assay, the worms were taken out of storage and re-suspended in trichloroacetic acid (10%, 50 μL). After re-suspension, the worms were immediately lysed in water bath sonicator (Soniclean, Thebarton, Australia) for 5 minutes. The water bath was kept cool using ice. Tubes were kept on ice for an additional 15 minutes before centrifugation at 15,000*g* at 4°C for 5 minutes. The supernatant and ATP standard were pipetted into a white 96-well plate, followed by an addition of arsenite ATP buffer. The ATP levels were measured using a luminometer (Infinite 200, Tecan, Männedorf, Switzerland) preprogrammed to inject 150-μL firefly lantern extract (2 mg/mL in water). The luminescence signal was integrated for 10 seconds.

Mitochondrial Copy Number Quantification

Mitochondrial copy number was quantified according to Schaffer and colleagues (13). Briefly, individual worms (*glp-1*) were transferred from NGM plates into polymerase chain reaction tubes containing 50 μL of lysis buffer. The worms were put through two cycles of freeze and thawed at −80°C in order to break their cuticle and to aid in the lysis process. Following the freeze thaw cycles, the worms were incubated at 60°C for 1 hour and 95°C for 10 minutes to inactivate proteinase K. Mitochondrial copy number of individual worms was determined using quantitative real-time polymerase chain reaction using standards where the copy number was known from serial dilution.

Protein Carbonyl Determination

Protein carbonyl determination was performed according to Schaffer and colleagues (13). A population of 200 worms (*glp-1*) was collected in M9 buffer in microfuge tubes and washed three times to remove any residual bacteria. The samples were re-suspended in 100 μL of phosphate-buffered saline with Tween-20 (0.1% Tween-20 in phosphate-buffer saline; 1st BASE, Science Park, Singapore) containing 1 mM of phenylmethylsulfonyl fluoride and sonicated on ice at 40% amplitude (Vibra-cell, Sonics & Materials, Newtown, CT) for 20 pulses, each lasting 5 seconds, with 1 second in between pulses. Protein concentrations of the samples were determined using the D_c-Protein Assay (Bio-Rad, Hercules, CA). Derivatization of the samples was performed as follows: 5 μL of worm lysate was added to 5 μL of 12% sodium dodecyl sulfate and 10 μL of 20 mM 2,4-dinitrophenylhydrazine and incubated for 15 minutes at room temperature. Afterwards, 7.5 μL of neutralization solution (2 M Tris, 30% glycerol) was added. Lysate containing 1 μg of protein was then loaded to a slot blot apparatus (Bio-Rad). Using vacuum, the proteins were transferred onto a nitrocellulose membrane (Bio-Rad). After blocking for nonspecific binding, the membrane was probed with anti-2,4-dinitrophenylhydrazine antibody (Chemicon International, Temecula, CA), followed by a secondary detection by horseradish peroxidase-conjugated anti-rabbit IgG antibody. All incubations were performed for 1 hour at room temperature. Antibody-bound proteins were detected by chemiluminescence using Chemidoc XRS imaging system (Bio-Rad, Milan, Italy). All chemicals and antibodies used in this assay were obtained from Oxyblot Protein Oxidation Detection Kit (Chemicon International).

Statistical Analysis

The mean lifespan calculation and the log-rank test were performed using OASIS (39). Statistical analyses for the rest of the data were performed on MATLAB (The MathWorks, Natick, MA). Significance of the mean was assessed using analysis of variance, and *p* values lesser than .05 (*) and .01 (**) were considered to be statistically significant.

Results

Lithium Leads to Increased Lifespan and Better Locomotor Phenotype

Cohorts of wild-type control worms (*glp-1*) were exposed to 10 mM of LiCl from Day 3 after bleaching. Treatment of 10 mM LiCl has been shown to reduce inositol levels (40) and provide the maximum increase of median lifespan in *C. elegans* (22). In this study, the LiCl treatment was found to result in approximately 10% increase in the mean lifespan, without any change in the maximum lifespan (see Figure 1A). The healthspan of lithium-treated worms

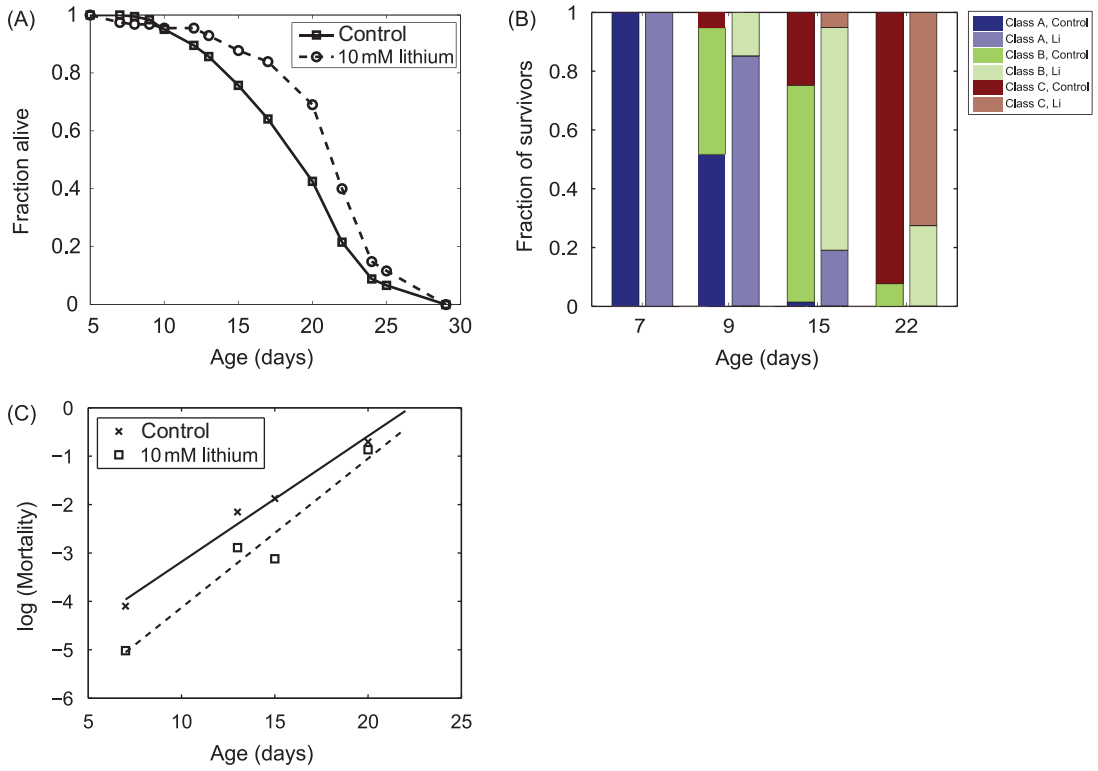

Figure 1. (**A**) Kaplan–Meier survival curves of JK1107 (*glp-1*) worms exposed to 10 mM of lithium chloride (LiCl). Scoring was conducted using randomized and blinded samples. The survival curves were found to be significantly different using a log-rank test ($p < .0001$). The mean lifespan for the control and lithium-treated worms are 19.56 days (95% CI [18.86, 20.26]) and 21.7 days (95% CI [20.96, 22.44]), respectively. (**B**) Motility phenotype of surviving worms. Surviving worms on each scoring day were classified into three motility phenotypes according to the study by Herndon and colleagues (36). Class A worms are constantly moving and respond strongly to prodding by moving away from stimulus. Class B worms are stationary unless prodded and leave behind tracks that are nonsinusoidal. Members of class C do not move when prodded, but only flex their head in response to stimulus. (**C**) Mortality rate of control and LiCl-treated worms. The mortality rate doubling time for the control and LiCl-treated worms were not statistically significantly different.

was also found to be better preserved, as shown by slower decline in locomotor phenotype at all ages in comparison to nontreated cohorts (see Figure 1B). The mortality rate doubling time was estimated by fitting the survival curve from Day 10 to Day 22 to the Gompertz function (37). The estimated mortality rate doubling time for control and LiCl-treated worms were 2.67 and 2.25 days, respectively (see Figure 1C). However, the difference in the mortality rate doubling time between the two groups was not statistically significant, indicating that lithium treatment did not significantly slow the rate of aging.

Lithium Induces the Formation of lgg-1:GFP Puncta in C. elegans Strain DA2123

The possible induction of autophagy in *C. elegans* by lithium was investigated using worm strain DA2123, carrying *lgg-1*:GFP (green fluorescent protein) fusion protein (41). As *lgg-1* is the worm ortholog of mammalian ubiquitin-like protein LC3, upon enhancement of autophagy, *lgg-1*:GFP should appear as puncta under a fluorescence microscope corresponding to preautophagosomal and autophagosomal structures (42). Exposure to 10 mM of LiCl for 12 hours during young adult life (Day 2) led to a statistically significant redistribution ($p < 10^{-4}$) of *lgg-1*:GFP from diffused to punctate foci (see Figure 2). The *p*-value was obtained from blinded scoring of the GFP images ($n = 70$). However, it should be noted that the appearance of *lgg-1*:GFP puncta could also increase if the later stages of the autophagy were suppressed. Because lithium has been previously shown to induce autophagy in mammalian cell culture by inhibiting inositol monophosphatase (24), we hypothesize that lithium induces autophagy in *C. elegans* and therefore the extension of lifespan and healthspan in lithium-treated worms was concomitant with the upregulation of autophagy.

Lithium Increases Mitochondrial Energetics but Lowers mtDNA Copy Number

To investigate if lithium treatment resulted in a better preservation of mitochondrial function with age, the ATP levels were measured in control and lithium-treated worms at different ages. Consistent with our previous study (43), control worms exhibited an age-related decrease in the ATP production (see Figure 3A). Although lithium-treated worms did not exhibit any significant change in the ATP level 24 hours after treatment (Day 4), the ATP levels of

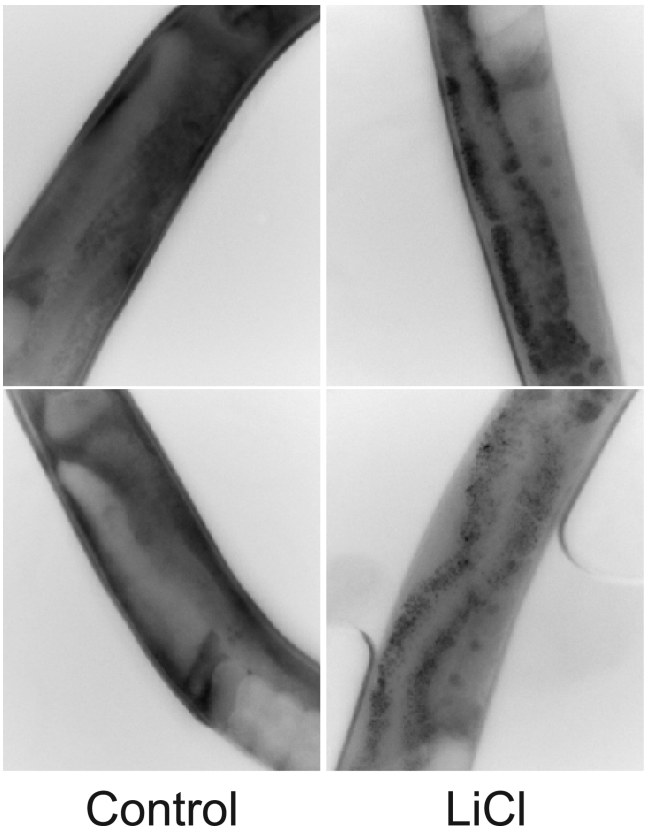

Figure 2. Cellular localization of *lgg-1*:GFP in intestinal cells of control (left column) and lithium chloride (LiCl)-treated worms at 10 mM of LiCl for 24 hours (right column). The punctuate foci distribution of *lgg-1*:GFP represents the preautophagosomal and autophagosomal structures.

Li-treated group were 72% and 53% higher than those of the control group on Day 8 and Day 14, respectively ($p < .01$). In addition, we measured the mtDNA copy number as a function of age from the two study groups, the result of which is presented in Figure 3B. Both groups showed an age-related decline in the mtDNA copy number. Lithium treatment increased the mtDNA amount by 12% at 24 hours after exposure ($p < .01$). Despite this initial increase, the mtDNA copy number in lithium-treated worms on Day 8 and Day 14 were 13% ($p < .05$) and 31% ($p < .01$) lower than that in control group, respectively (see Figure 3B).

Lithium Treatment Does Not Affect Oxidative Protein Damage

Age-related decline in autophagy has been proposed to be an important factor contributing to the accumulation of oxidative damaged macromolecules (12). Therefore, we determined levels of total protein carbonyl content (PCC), a marker of global oxidative protein damage in control and lithium-treated worms. Both groups showed a similar age-dependent increase in the oxidative damage. However, the PCC levels of the lithium-treated worms were not statistically different from the control group (see Figure 3C).

Population Balance Model of Mitochondria

In order to better understand how lithium may improve mitochondrial function, we propose a mathematical model that describes the population of functional and dysfunctional mitochondria. The model equations are given as follows:

$$\frac{dM_F}{dt} = V_b - k_a M_F - k_d M_F \quad (1)$$

$$\frac{dM_D}{dt} = -\alpha k_a M_D + k_d M_F \quad (2)$$

The first equation describes the population balance of functional mitochondria M_F, where M_F is generated by mitochondrial biogenesis at a rate of V_b, and removed by mitophagy and damage with rate constants of k_a and k_d, respectively. Similarly, the population of dysfunctional mitochondria M_D is affected by their removal through mitophagy and generation through damage process. Mitophagy is modeled to be selective, as (dysfunctional) mitochondria with lowered membrane potential have been shown to be preferentially removed (44). Specifically, the mitophagy of M_D is scaled by a factor $\alpha > 1$. The model equations described above are general enough to describe both selective and nonselective autophagy of dysfunctional

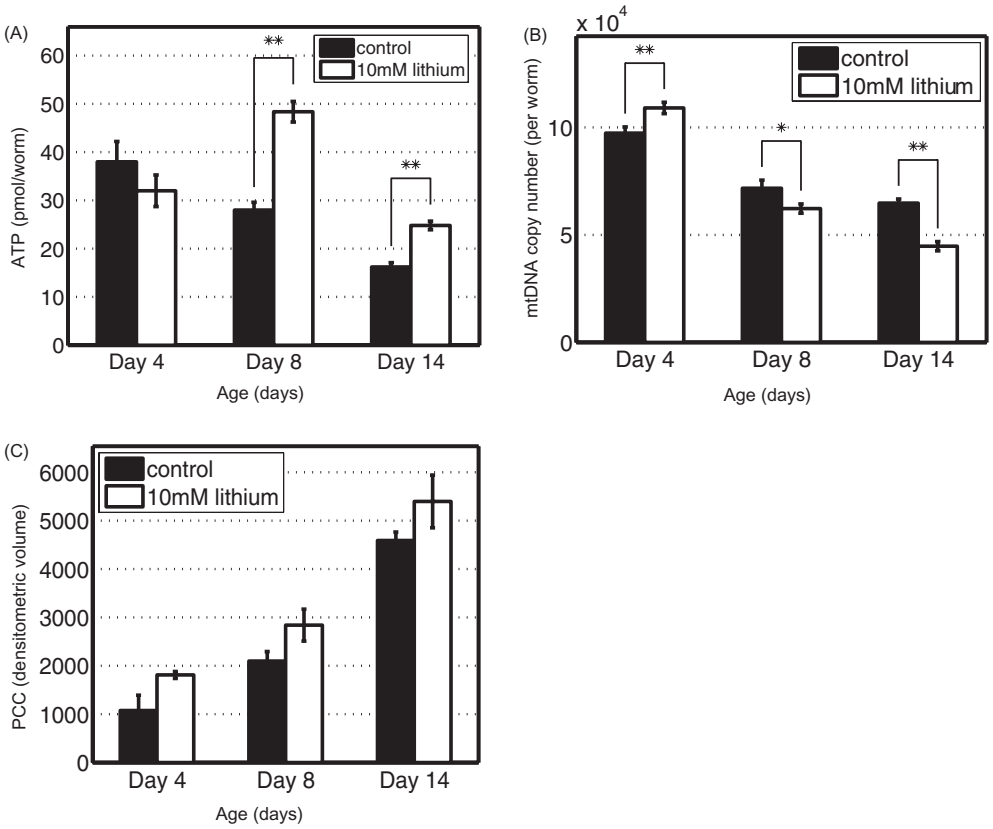

Figure 3. (**A**) Mean adenosine triphosphate (ATP) levels on Days 4, 8, and 14 for control and lithium chloride (LiCl)-treated worms (**$p < .01$). (**B**) Age-dependent decline in mean mitochondrial DNA copy number in control and LiCl-treated worms (*$p < .05$, **$p < .01$). (**C**) Age-dependent increase in protein carbonyl content (PCC) in control and LiCl-treated worms. The mean PCC levels between the control and lithium-treated worms were not significantly different (Day 4: $p = .09$; Day 8: $p = .13$; Day 14: $p = .23$, by analysis of variance). These assays were performed for three biological repeats, and for the PCC, each biological repeat corresponds to the average of three technical repeats. The error bars indicate the standard deviation of the mean.

mitochondria, in which case the parameter α denotes the effective increase in the autophagy due to selectivity.

The steady-state population can be obtained by setting the time derivatives in equations (1) and (2) to 0, resulting in the following algebraic equations:

$$M_{F,s} = \frac{V_b / k_a}{1 + k_d / k_a} \tag{3}$$

$$M_{D,s} = \frac{k_d}{\alpha k_a} M_{F,s} = \frac{V_b / k_a}{\alpha} \left(\frac{k_d / k_a}{1 + k_d / k_a} \right) \tag{4}$$

where the subscript s denotes steady-state condition. The total population of mitochondria at steady state $M_{T,s}$ is simply the sum:

$$M_{T,s} = M_{F,s} + M_{D,s} = \frac{V_b}{k_a} - (\alpha - 1) M_{D,s} \tag{5}$$

The model was implemented in MATLAB. The steady-state values of mitochondrial populations were computed using the parameter ranges in Table 1.

Table 1. Model Parameters

Parameter	Range of Values	Remarks
α	3–24	Autophagosome formation was observed between 1 and 8 h for depolarized mitochondria and ~24 h for normal mitochondria (45).
V_b / k_a	50–200	The ratio was based on an average number of mitochondria per cell of 80 (46).
k_d / k_a	0.1–3	

There are a few immediate implications from the model regarding how steady-state mitochondria population varies with changes in the biogenesis, mitophagy, and damage rates. First, the steady-state population of mitochondria ($M_{F,s}$,$M_{D,s}$, and $M_{T,s}$) depends linearly on the relative balance between biogenesis and mitophagy V_b / k_a (see Table 1), and not on the turnover rate constants V_b and k_a, the values of which are still uncertain (47). When the damage rate becomes higher, that is, increasing k_d / k_a, $M_{D,s}$ will expectedly rise (see equation 2). However, because

mitophagy is selective ($\alpha > 1$), higher $M_{D,s}$ will lead to an increase in the overall mitophagy activity and, therefore, a decrease in $M_{T,s}$ as suggested by equation (5). Note that in absence of selectivity in mitophagy ($\alpha = 1$), $M_{T,s}$ depends only on V_b / k_a.

Discussion

The reduction of mtDNA in Li-treated group at older ages is perhaps not unexpected in light of the upregulation of autophagy. But, the improvement in the ATP levels in Li-treated cohort over control, despite the drop in the mtDNA copy number, suggests that lithium can boost the overall energetics of the mitochondrial population in *C. elegans*. We rely on a trend analysis of the mitochondrial population model to explain and better understand the effects of lithium. In the model analysis, the aging process and lithium are assumed to cause changes in the model parameters (ie, V_b, k_a, and k_d). We make the assumptions that (a) age-related parameter drifts occur slowly enough such that the mitochondrial populations can be approximated by their steady-state values (pseudo-steady-state assumption) and (b) the parameter change due to lithium occurs instantaneously when compared with the parameter drift due to aging. By these assumptions, the number of functional, dysfunctional, and total mitochondria can be computed using equations (3)–(5). Figure 4A and B show the contour lines of total and dysfunctional mitochondria at steady state as a function of the parameter ratios V_b / k_a and k_d / k_a based on these model equations. In the following analysis, we also assume that the number of mtDNA in a single mitochondrion remains roughly constant, such that an increase in the mtDNA copy number corresponds to an increase in the mitochondrial number. This assumption is based on studies showing that the occurrence of large mitochondria is rare (48–50), and larger mitochondria are more likely to undergo mitochondrial fission (51).

As mentioned earlier, aging has been associated with a decline in mitochondrial biogenesis and autophagy (10,52,53) and an increase in oxidative damage (12,54) (also see Figure 3C). Following these observations, we have drawn the direction of age-related parameter drift on Figure 4A (control arrow) such that V_b / k_a is maintained constant, but k_d / k_a increases. According to equations (3) and (4), higher k_d / k_a without any change in V_b / k_a will lead to a smaller population of functional mitochondria $M_{F,s}$ and a larger population of dysfunctional mitochondria $M_{D,s}$, as shown in Figure 4B. Due to the selectivity of mitophagy, larger $M_{D,s}$ means a higher overall mitophagy rate, and by equation (5), the total mitochondria $M_{T,s}$ is expected to drop. Figure 4A shows that the aging parameter drift corresponds to a decrease in $M_{T,s}$, in agreement with our experimental data showing decreasing mtDNA copy number with age. Note that any parameter drift in the same general direction of increasing k_d / k_a is associated with a lower total mitochondria, that is, the assumption that V_b / k_a remains constant with aging can be relaxed.

In order to draw the age-related parameter drift for lithium-treated worms, we observe that (A) lithium upregulated

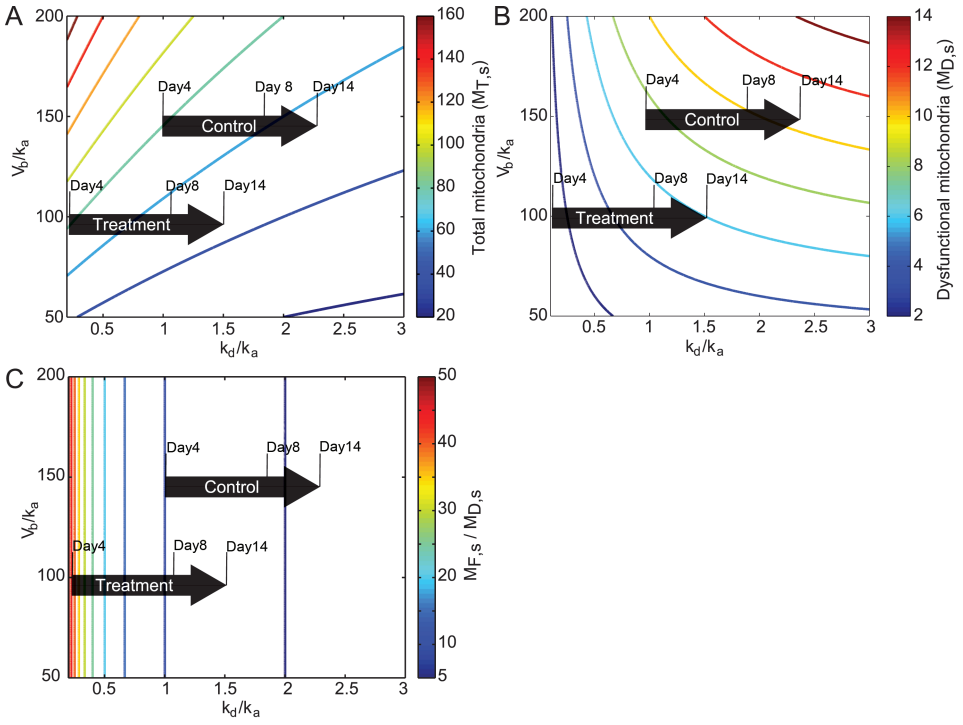

Figure 4. Contour lines of (**A**) total mitochondria $M_{T,s}$, (**B**) dysfunctional mitochondria, and (**C**) the ratio of functional to dysfunctional mitochondria $M_{F,s} / M_{D,s}$, using $\alpha = 10$. The arrows show the postulated parameter drift associated with aging in the control and Li-treated worms.

autophagy (Figure 2), (B) lithium did not affect the PCC levels (Figure 3C), and (C) lithium led to a small increase in the mtDNA copy number initially (Day 4), but caused a faster age-related decrease (Figure 3B). Observation A implies that lithium-treated worms should have a higher k_a than the control, while observation B suggests that the parameter k_d should remain roughly the same as the control. Therefore, the ratio k_d / k_a and possibly V_b / k_a of the treatment group should be smaller than that of the control at the same ages. Although intuition suggests that enhancement of autophagy by lithium should lead to fewer mitochondria, our experimental data on mtDNA copy number indicated otherwise, at least initially.

The model can be used to give an explanation for this counterintuitive observation. When k_d / k_a is lowered, the ratio $M_{F,s} / M_{D,s}$ given by

$$\frac{M_{F,s}}{M_{D,s}} = \frac{\alpha}{k_d / k_a} \tag{6}$$

will increase (see Figure 4C). In other words, upregulating autophagy will shift the mitochondria population to be more functional, and the magnitude of this shift scales with the selectivity of mitophagy. Consequently, as functional mitochondria are removed at a slower rate than dysfunctional ones, increasing mitophagy may not necessarily lead to more removal of mitochondria (functional/dysfunctional) and to a smaller mitochondrial population $M_{T,s}$. As shown in Figure 4A (Day 4 worms, Li-treated vs control worms), for an appropriately chosen V_b / k_a and following observation C, the two contradicting forces can cancel out. Although lithium treatment has been associated with the upregulation of both mitochondrial biogenesis and autophagy, the lower V_b / k_a ratio indicates that mitophagy is influenced more strongly than biogenesis.

The age-related parameter drift in the lithium-treated worms is drawn in Figure 4 by copying the drift of the control group, starting from a lower k_d / k_a and V_b / k_a values. Figure 4A shows a faster age-related drop in $M_{T,s}$ for the Li-treated group, reproducing the mtDNA data in Figure 3B (observation C). This model prediction can be explained by looking at equation (4), which suggests that the effect of increasing k_d / k_a on $M_{D,s}$ diminishes with higher k_d / k_a (see the term in brackets in equation 4). At very high k_d / k_a, most mitochondria are already dysfunctional and increasing k_d / k_a further will not lead to proportionally higher $M_{D,s}$. Because lithium lowers k_d / k_a, the aging parameter drift for lithium-treated worms corresponds to a higher increase in $M_{D,s}$ and thus, a faster decrease in $M_{T,s}$ with age (see Figure 4A and B). Nevertheless, it should be noted that under lithium treatment, $M_{D,s}$ is always lower than that of control (see Figure 4B). Therefore, the higher increase in $M_{D,s}$ with aging for Li-treated group should not be viewed as an acceleration of mitochondrial dysfunction, but rather as a consequence of the shift in the proportions of functional and dysfunctional mitochondria.

Currently, there is no experimental data that can directly specify the age-related changes in the mitochondrial biogenesis, autophagy, and damage rates in control and lithium-treated worms. Nevertheless, the contour lines of the total mitochondria $M_{T,s}$ in Figure 4A are more compressed in the region with lower k_d / k_a and V_b / k_a values, indicating higher sensitivity of $M_{T,s}$ to changes in the parameter values. We note that the higher sensitivity is proportional to the strength of selectivity of mitophagy (α values, see equation 5). Therefore, the insight from our model, where in lithium-treated worms, the faster drop in the total mitochondria is due to the population shift to functional mitochondria, does not depend on how the age-related parameter drifts were drawn for these worms.

The cellular ATP is an indicator of the respiratory capacity of the cell. The most straightforward assumption using the number of functional mitochondria $M_{F,s}$ as a metric of cellular respiratory function could not explain the ATP increase by lithium. The population of functional mitochondria closely resembles $M_{T,s}$, where $M_{F,s}$ drops with increasing k_d / k_a (see Supplementary Figure S1). Therefore, we explain the ATP increase by relating the mitochondrial respiratory capacity to the ratio of functional and dysfunctional mitochondria (see equation 6). Figure 4C shows the contour line of the ratio $M_{F,s} / M_{D,s}$ as a function of V_b / k_a and k_d / k_a. We have duplicated the age-related parameter drifts for control and lithium-treated groups from Figure 4A to Figure 4C. Except for Day 4, the changes in $M_{F,s} / M_{D,s}$ in the direction of the age-related parameter drifts are consistent with the upregulation of ATP by lithium (on Days 8 and 14).

The deviation on Day 4 is perhaps not unexpected as the complete effects of lithium on mitochondrial population and cellular energetics may require more than 1 day. For example, in bovine endothelial cells, mitochondrial mass, transcription factors related to mitochondrial biogenesis, oxidative phosphorylation components, and ATP levels continue to increase between 24 and 36 hours of lithium exposure (33). Unfortunately, we are not aware of any tool to directly measure the ratio of $M_{F,s} / M_{D,s}$ in *C. elegans*, and thus, the outcome of the model analysis could not be directly validated. Nevertheless, the importance of the ratio of $M_{F,s} / M_{D,s}$, not $M_{F,s}$, in the production of ATP is consistent with observations in aged skeletal muscle, in which oxidative phosphorylation deficiency in atrophied muscle fiber correlated with a low ratio of wild-type to mutant mtDNA and not with the amount of wild-type mtDNA (55). Hence, the model analysis suggests that the cell benefits from the selectivity of mitophagy ($\alpha > 1$), as upregulation of autophagy can boost the $M_{F,s} / M_{D,s}$ ratio and ATP production. In addition, the benefit of lithium comes at a cost of having a smaller mitochondrial population. When the number of functional mitochondria becomes too small, below a certain threshold, we expect that the ATP improvement cannot be sustained, regardless of the ratio $M_{F,s} / M_{D,s}$.

It is to some degree possible to counter the decline in mitochondrial function with age through life-style interventions such as exercise and calorie restriction, both of which have been shown to upregulate the expression of PGC-1α (56) and mitophagy, thereby increasing mitochondrial turnover (57). Endurance exercise has also been shown to prevent mtDNA depletion and mutations, increase mitochondrial oxidative capacity and respiratory chain assembly, and even prevent premature death and progeroid aging in mtDNA mutator mice (58). However, exercise could neither slow the age-related decline in mtDNA copy number and the expression of mitochondrial respiratory genes nor increase the maximum lifespan of rats (59). Nevertheless, the population of mitochondria could tilt toward a higher functional to dysfunctional ratio as a result of exercise, which similar to the lithium treatment here, would lead to a better preservation of mitochondrial function with age. On the other hand, calorie restriction has been found to slow the age-related decline in PGC-1α expression (60), improve mitochondrial activity in the skeletal muscle of aged animals (but not young ones) (60,61), and to increase the maximum lifespan in a range of organisms (from yeast to rats) (62).

Conclusion

In this study, LiCl treatment has been shown to positively influence the lifespan and healthspan of *C. elegans*. The extension of median lifespan and healthspan was accompanied by improvements in mitochondrial energetics, as indicated by an increase in the ATP levels. Our experimental study showed that lithium exposure upregulated autophagy. This increase was not associated with any significant change in the global oxidative damage level. Interestingly, the improvement in mitochondrial energetics was accompanied by a decrease in the mtDNA copy number with age. In order to provide an explanation for these observations, a population balance model of mitochondria was formulated, describing how the numbers of functional and dysfunctional mitochondria and their ratio were affected by mitochondrial biogenesis, selective mitophagy, and mitochondrial damage process. A trend analysis of this model was subsequently performed based on current understanding and our experimental observations. The analysis suggested that (a) lithium elicits a greater increase in autophagy than in mitochondrial biogenesis, (b) the cellular respiratory capacity is correlated with the ratio of functional and dysfunctional mitochondria, and (c) the increase in the ATP levels by lithium is due to a higher ratio of functional to dysfunctional mitochondria. One corollary from the model analysis was that the improvement in the mitochondrial respiratory function by upregulating selective mitophagy might be associated with a cost in terms of lowered mitochondrial population size. The model trend analysis thus offered a simple-yet-elegant explanation on how increasing (selective) autophagy by lithium could improve mitochondrial energetics.

Supplementary Material

Supplementary material can be found at: http://biomedgerontology.oxfordjournals.org/

Funding

This work was supported by ETH Zurich and the Ministry of Education, Singapore (MOE2010-T2-2–048).

References

1. Troen BR. The biology of aging. *Mt Sinai J Med*. 2003;70:3–22.
2. Brunk UT, Terman A. The mitochondrial-lysosomal axis theory of aging: accumulation of damaged mitochondria as a result of imperfect autophagocytosis. *Eur J Biochem*. 2002;269:1996–2002. doi:10.1046/j.1432-1033.2002.02869.x
3. Holliday R. The multiple and irreversible causes of aging. *J Gerontol A Biol Sci Med Sci*. 2004;59:B568–B572. doi:10.1093/gerona/59.6.B568
4. Ryan MT, Hoogenraad NJ. Mitochondrial-nuclear communications. *Annu Rev Biochem*. 2007;76:701–722. doi:10.1146/annurev.biochem.76.052305.091720
5. Figueiredo PA, Powers SK, Ferreira RM, Appell HJ, Duarte JA. Aging impairs skeletal muscle mitochondrial bioenergetic function. *J Gerontol A Biol Sci Med Sci*. 2009;64:21–33. doi:10.1093/gerona/gln048
6. Short KR, Bigelow ML, Kahl J, et al. Decline in skeletal muscle mitochondrial function with aging in humans. *Proc Natl Acad Sci U S A*. 2005;102:5618–5623. doi:10.1073/pnas.0501559102
7. Kujoth GC, Hiona A, Pugh TD, et al. Mitochondrial DNA mutations, oxidative stress, and apoptosis in mammalian aging. *Science*. 2005;309:481–484. doi:10.1126/science.1112125
8. Cuervo AM, Dice JF. Age-related decline in chaperone-mediated autophagy. *J Biol Chem*. 2000;275:31505–31513. doi:10.1074/jbc.M002102200
9. Wohlgemuth SE, Seo AY, Marzetti E, Lees HA, Leeuwenburgh C. Skeletal muscle autophagy and apoptosis during aging: effects of calorie restriction and life-long exercise. *Exp Gerontol*. 2010;45:138–148. doi:10.1016/j.exger.2009.11.002
10. Derbré F, Gomez-Cabrera MC, Nascimento AL, et al. Age associated low mitochondrial biogenesis may be explained by lack of response of PGC-1α to exercise training. *Age (Dordr)*. 2012;34:669–679. doi:10.1007/s11357-011-9264-y
11. Liu D, Sartor MA, Nader GA, et al. Microarray analysis reveals novel features of the muscle aging process in men and women. *J Gerontol A Biol Sci Med Sci*. 2013;68:1035–1044. doi:10.1093/gerona/glt015
12. Terman A, Gustafsson B, Brunk UT. Autophagy, organelles and ageing. *J Pathol*. 2007;211:134–143. doi:10.1002/path.2094
13. Schaffer S, Gruber J, Ng LF, et al. The effect of dichloroacetate on health- and lifespan in *C. elegans*. *Biogerontology*. 2011;12:195–209. doi:10.1007/s10522-010-9310-7
14. Gruber J, Fong S, Chen CB, et al. Mitochondria-targeted antioxidants and metabolic modulators as pharmacological interventions to slow ageing. *Biotechnol Adv*. 2013;31:563–592. doi:10.1016/j.biotechadv.2012.09.005
15. Menshikova EV, Ritov VB, Fairfull L, Ferrell RE, Kelley DE, Goodpaster BH. Effects of exercise on mitochondrial content and function in aging human skeletal muscle. *J Gerontol A Biol Sci Med Sci*. 2006;61:534–540. doi:10.1093/gerona/61.6.534
16. Kelly DP, Scarpulla RC. Transcriptional regulatory circuits controlling mitochondrial biogenesis and function. *Genes Dev*. 2004;18:357–368. doi:10.1101/gad.1177604
17. Wenz T, Diaz F, Spiegelman BM, Moraes CT. Activation of the PPAR/PGC-1alpha pathway prevents a bioenergetic deficit and effectively improves a mitochondrial myopathy phenotype. *Cell Metab*. 2008;8:249–256. doi:10.1016/j.cmet.2008.07.006

18. Stroikin Y, Dalen H, Lööf S, Terman A. Inhibition of autophagy with 3-methyladenine results in impaired turnover of lysosomes and accumulation of lipofuscin-like material. *Eur J Cell Biol*. 2004;83:583–590. doi:10.1078/0171-9335-00433
19. Zhou R, Yazdi AS, Menu P, Tschopp J. A role for mitochondria in NLRP3 inflammasome activation. *Nature*. 2011;469:221–225. doi:10.1038/nature09663
20. Hara T, Nakamura K, Matsui M, et al. Suppression of basal autophagy in neural cells causes neurodegenerative disease in mice. *Nature*. 2006;441:885–889. doi:10.1038/nature04724
21. Ravikumar B, Vacher C, Berger Z, et al. Inhibition of mTOR induces autophagy and reduces toxicity of polyglutamine expansions in fly and mouse models of Huntington disease. *Nat Genet*. 2004;36:585–595. doi:10.1038/ng1362
22. McColl G, Killilea DW, Hubbard AE, Vantipalli MC, Melov S, Lithgow GJ. Pharmacogenetic analysis of lithium-induced delayed aging in *Caenorhabditis elegans*. *J Biol Chem*. 2008;283:350–357. doi:10.1074/jbc.M705028200
23. Harrison DE, Strong R, Sharp ZD, et al. Rapamycin fed late in life extends lifespan in genetically heterogeneous mice. *Nature*. 2009;460:392–395. doi:10.1038/nature08221
24. Sarkar S, Floto RA, Berger Z, et al. Lithium induces autophagy by inhibiting inositol monophosphatase. *J Cell Biol*. 2005;170:1101–1111. doi:10.1083/jcb.200504035
25. Klionsky DJ, Emr SD. Autophagy as a regulated pathway of cellular degradation. *Science*. 2000;290:1717–1721. doi:10.1126/science.290.5497.1717
26. Yatham LN. Atypical antipsychotics for bipolar disorder. *Psychiatr Clin North Am*. 2005;28:325–347. doi:10.1016/j.psc.2005.01.001
27. Quiroz JA, Machado-Vieira R, Zarate CA Jr, Manji HK. Novel insights into lithium's mechanism of action: neurotrophic and neuroprotective effects. *Neuropsychobiology*. 2010;62:50–60. doi:10.1159/000314310
28. Young W. Review of lithium effects on brain and blood. *Cell Transplant*. 2009;18:951–975. doi:10.3727/096368909X471251
29. Wang Q, Xu X, Li J, et al. Lithium, an anti-psychotic drug, greatly enhances the generation of induced pluripotent stem cells. *Cell Res*. 2011;21:1424–1435. doi:10.1038/cr.2011.108
30. Senatorov VV, Ren M, Kanai H, Wei H, Chuang DM. Short-term lithium treatment promotes neuronal survival and proliferation in rat striatum infused with quinolinic acid, an excitotoxic model of Huntington's disease. *Mol Psychiatry*. 2004;9:371–385. doi:10.1038/sj.mp.4001463
31. Chuang DM, Chen RW, Chalecka-Franaszek E, et al. Neuroprotective effects of lithium in cultured cells and animal models of diseases. *Bipolar Disord*. 2002;4:129–136. doi:10.1034/j.1399-5618.2002.01179.x
32. Harris H, Rubinsztein DC. Control of autophagy as a therapy for neurodegenerative disease. *Nat Rev Neurol*. 2012;8:108–117. doi:10.1038/nrneurol.2011.200
33. Struewing IT, Barnett CD, Tang T, Mao CD. Lithium increases PGC-1alpha expression and mitochondrial biogenesis in primary bovine aortic endothelial cells. *FEBS J*. 2007;274:2749–2765. doi:10.1111/j.1742-4658.2007.05809.x
34. Zarse K, Terao T, Tian J, Iwata N, Ishii N, Ristow M. Low-dose lithium uptake promotes longevity in humans and metazoans. *Eur J Nutr*. 2011;50:387–389. doi:10.1007/s00394-011-0171-x
35. Stiernagle T. Maintenance of *C. elegans*. *WormBook*. 2006:1–11.
36. Herndon LA, Schmeissner PJ, Dudaronek JM, et al. Stochastic and genetic factors influence tissue-specific decline in ageing *C. elegans*. *Nature*. 2002;419:808–814. doi:10.1038/nature01135
37. de Magalhães JP, Curado J, Church GM. Meta-analysis of age-related gene expression profiles identifies common signatures of aging. *Bioinformatics*. 2009;25:875–881. doi:10.1093/bioinformatics/btp073
38. Shaham S. Methods in cell biology. In: Community TCeR, Wormbook, ed. *WormBook*. Pasadena, CA. 2006; http://www.wormbook.org. doi:10.1895/wormbook.1.49.1
39. Yang JS, Nam HJ, Seo M, et al. OASIS: online application for the survival analysis of lifespan assays performed in aging research. *PLoS One*. 2011;6:e23525. doi:10.1371/journal.pone.0023525
40. Williams RS, Cheng L, Mudge AW, Harwood AJ. A common mechanism of action for three mood-stabilizing drugs. *Nature*. 2002;417:292–295. doi:10.1038/417292a
41. Kang C, You YJ, Avery L. Dual roles of autophagy in the survival of *Caenorhabditis elegans* during starvation. *Genes Dev*. 2007;21:2161–2171. doi:10.1101/gad.1573107
42. Meléndez A, Tallóczy Z, Seaman M, Eskelinen EL, Hall DH, Levine B. Autophagy genes are essential for dauer development and life-span extension in *C. elegans*. *Science*. 2003;301:1387–1391. doi:10.1126/science.1087782
43. Gruber J, Ng LF, Fong S, et al. Mitochondrial changes in ageing *Caenorhabditis elegans*–what do we learn from superoxide dismutase knockouts? *PLoS One*. 2011;6:e19444. doi:10.1371/journal.pone.0019444
44. Twig G, Elorza A, Molina AJA, et al. Fission and selective fusion govern mitochondrial segregation and elimination by autophagy. *EMBO J*. 2008;27:433–446. doi:10.1038/sj.emboj.7601963
45. Robin ED, Wong R. Mitochondrial DNA molecules and virtual number of mitochondria per cell in mammalian cells. *J Cell Physiol*. 1988;136:507–513.
46. Safdar A, Bourgeois JM, Ogborn DI, et al. Endurance exercise rescues progeroid aging and induces systemic mitochondrial rejuvenation in mtDNA mutator mice. *Proc Natl Acad Sci USA*. 2011;108:4135–4140. doi:10.1073/pnas.1019581108
47. Poovathingal SK, Gruber J, Lakshmanan L, Halliwell B, Gunawan R. Is mitochondrial DNA turnover slower than commonly assumed? *Biogerontology*. 2012;13:557–564. doi:10.1007/s10522-012-9390-7
48. Twig G, Graf SA, Wikstrom JD, et al. Tagging and tracking individual networks within a complex mitochondrial web with photoactivatable GFP. *Am J Physiol Cell Physiol*. 2006;291:C176–C184. doi:10.1152/ajpcell.00348.2005
49. Huang B, Jones SA, Brandenburg B, Zhuang X. Whole-cell 3D STORM reveals interactions between cellular structures with nanometer-scale resolution. *Nat Methods*. 2008;5:1047–1052. doi:10.1038/nmeth.1274
50. Satoh M, Kuroiwa T. Organization of multiple nucleoids and DNA molecules in mitochondria of a human cell. *Exp Cell Res*. 1991;196:137–140. doi:10.1016/0014-4827(91)90467-9
51. Berman SB, Chen YB, Qi B, et al. Bcl-x L increases mitochondrial fission, fusion, and biomass in neurons. *J Cell Biol*. 2009;184:707–719. doi:10.1083/jcb.200809060
52. Donati A, Cavallini G, Paradiso C, et al. Age-related changes in the autophagic proteolysis of rat isolated liver cells: effects of antiaging dietary restrictions. *J Gerontol A Biol Sci Med Sci*. 2001;56:B375–B383. doi:10.1093/gerona/56.9.B375
53. Kaushik S, Arias E, Kwon H, et al. Loss of autophagy in hypothalamic POMC neurons impairs lipolysis. *EMBO Rep*. 2012;13:258–265. doi:10.1038/embor.2011.260
54. Figueiredo PA, Powers SK, Ferreira RM, Amado F, Appell HJ, Duarte JA. Impact of lifelong sedentary behavior on mitochondrial function of mice skeletal muscle. *J Gerontol A Biol Sci Med Sci*. 2009;64:927–939. doi:10.1093/gerona/glp066
55. Durham SE, Samuels DC, Cree LM, Chinnery PF. Normal levels of wild-type mitochondrial DNA maintain cytochrome c oxidase activity for two pathogenic mitochondrial DNA mutations but not for m.3243A–>G. *Am J Hum Genet*. 2007;81:189–195. doi:10.1086/518901
56. Konopka AR, Suer MK, Wolff CA, Harber MP. Markers of human skeletal muscle mitochondrial biogenesis and quality control: effects of age and aerobic exercise training. *J Gerontol A Biol Sci Med Sci*. 2013. doi:10.1093/gerona/glt107
57. Narendra D, Tanaka A, Suen DF, Youle RJ. Parkin is recruited selectively to impaired mitochondria and promotes their autophagy. *J Cell Biol*. 2008;183:795–803. doi:10.1083/jcb.200809125

58. Finley LW, Haigis MC. The coordination of nuclear and mitochondrial communication during aging and calorie restriction. *Ageing Res Rev.* 2009;8:173–188. doi:10.1016/j.arr.2009.03.003
59. Holloszy JO. Exercise increases average longevity of female rats despite increased food intake and no growth retardation. *J Gerontol*. 1993;48:B97–B100. doi:10.1093/geronj/48.3.B97
60. Baker DJ, Betik AC, Krause DJ, Hepple RT. No decline in skeletal muscle oxidative capacity with aging in long-term calorically restricted rats: effects are independent of mitochondrial DNA integrity. *J Gerontol A Biol Sci Med Sci*. 2006;61:675–684.
61. Hepple RT, Baker DJ, McConkey M, Murynka T, Norris R. Caloric restriction protects mitochondrial function with aging in skeletal and cardiac muscles. *Rejuvenation Res*. 2006;9:219–222. doi:10.1089/rej.2006.9.219
62. Masoro EJ. Overview of caloric restriction and ageing. *Mech Ageing Dev*. 2005;126:913–922. doi:10.1016/j.mad.2005.03.012